IEEE Access
Multidisciplinary ⋮ Rapid Review ⋮ Open Access Journal

Received 10 June 2024, accepted 31 July 2024, date of publication 6 August 2024, date of current version 27 August 2024.

Digital Object Identifier 10.1109/ACCESS.2024.3439474

RESEARCH ARTICLE

Automatic Mass Balancing of a Small Spherical Simulator for Attitude Control Verification

JAIME GERSON CUBA MAMANI[1], XINSHENG WANG[2], AND PABLO RAUL YANYACHI[1,3], (Senior Member, IEEE)

[1]School of Electronic Engineering, Universidad Nacional de San Agustín de Arequipa, Arequipa 04000, Peru
[2]Department of Astronautics, Beihang University, Beijing 100191, China
[3]Instituto de Investigación Astronómico y Aeroespacial Pedro Paulet, Universidad Nacional de San Agustín de Arequipa, Arequipa 04000, Peru

Corresponding author: Pablo Raul Yanyachi (raulpab@unsa.edu.pe)

This work was supported by the National Program of Scientific Research and Advanced Studies (PROCIENCIA) under Grant PE501079885-2022.

ABSTRACT In the aerospace field, researchers and engineers have been using attitude simulators to test and evaluate spacecraft attitude control algorithms, usually developed at the design stage. Moreover, thanks to the new technological achievements, small satellites can include more complex algorithms in their attitude determination and control systems. In consequence, the development of an attitude simulator that is able to perform different control algorithms with high attitude accuracy and stability is in high demand. In this paper, an automatic balancing method, along with a modified Model Reference Adaptive Control architecture for an uncertain dynamical system with unknown perturbation, was developed to address uncertainty suppression and disturbance rejection for an air-bearing spherical attitude simulator. The main feature of the proposed scheme consists of obtaining estimates of the offset vector generated by an unbalanced mass system in order to reduce it by moving small masses along each principal axis, ensuring stability and improving motion performance with an adaptive controller with input error modification. Simulation results were conducted according to the parameters for a small satellite 1U-class CubeSat platform inside a spherical structure.

INDEX TERMS Automatic mass balancing, model reference adaptive controller, attitude control, Euler parameters, spherical testbed.

I. INTRODUCTION

Following the current advances in hardware and software, the next generation of attitude estimation and control algorithms used in orbiting small satellites should include more complex algorithms for improved attitude stabilization and tracking with higher accuracy and stability. For decades, attitude simulators have been great resources for testing, verification and experimental validation of spacecraft attitude determination and control algorithms. The orbit-like environment offered by attitude simulators at ground facilities allows researchers, engineers, and students to test more complex algorithms that are not allowable to perform in orbit because of the implications in safety and cost.

The air-bearing testbed is the most common simulator used for attitude control verification, where a spacecraft simulator is suspended in an almost free-torque perturbation. The four types of disturbance present in the simulator are classified as the ones arising from the air bearing, the system, platform, the test system, and the environment [1]. Generally, a disturbance generated by the gravitational force is the most significant disturbance for an unbalanced mass system. In practice, this gravitational torque is hard to eliminate manually due to the pendulum-like motion of an offset vector generated by the distance between the Center of Mass (CM) and the Center of Rotation (CR) of the simulator platform. If this disturbance is not reduced properly, high torque as control input may be required to counteract the external disturbance.

In the literature, different methods have been proposed to deal with the unbalanced mass disturbance torque; for example, Sharifi proposed a mass identification

The associate editor coordinating the review of this manuscript and approving it for publication was Bin Xu.

characteristic for an automatic mass balancing system using Leverngerg-Marquardt optimization method [2]. Schwartz proposed a batch system identification technique for the full nonlinear equation of motion of the system [3]. Chesi proposed an adaptive nonlinear feedback control method for an automatic mass balancing system [4]. Kim proposed a batch least-square method for estimating inertial properties for an automatic mass balancing system [5]. Kim in [6] presented an adaptive control law for an automatic balancing method in a spherical air-bearing simulator where the gravitational disturbance was determined by the rate of change of the total momentum in the control moment gyro array. Then, an adaptive controller, with sufficient excitation, for an online compensation of the center of gravity offset was adopted. Between these methods, the most effective and implemented one are the ones with a batch least-square estimation method for an automatic mass balancing system.

A comparison between parameter estimation methods and balancing methods for spacecraft simulators can be found in the review made by Cardoso [7]. The review presents the pros and cons of these methods and concludes that the main problem related to the development of an attitude simulator was in its calibration. Modenini compared system performance between some testbeds, aiming to describe design solutions for developing a dynamic nanosatellite attitude simulator [8].

A control method in presence of nonlinearities, parameter uncertain, and constraints for an attitude simulator can be found in Jamshidi [9]. Malekzadeh proposed a modified feedback linearization controller using sliding-mode observers to estimate angular velocity [10].

Hardware implementation of augmented mass balancing systems can be found in [11], [12], [13], and [14], where air-bearing testbeds are combined with other systems like Helmholtz coils and sun sensor simulators, so that, the simulated environment conditions can meet real orbit scenarios for testing different attitude estimation and control algorithms for small satellites.

According to [4], [6], [8], and [15], the disturbance torque acting on an air-bearing, for a small satellite, must be reduced to a torque factor below 10^{-5} N-m for an orbit-like simulation of the Low Earth Orbit. While this task is hard to achieve, an approximated and acceptable result can be obtained by balancing the simulator platform through moving masses and changing the center of mass of the simulator platform to a position near the center of rotation of the air-bearing testbed. The balancing method can be done manually or automatically, being the last one more accurate, faster and with less effort [7].

According to [16], the goal of balancing the simulator platform is to increase the period of oscillations by considering the system's stability. In their research, Young first identified the mass offset vector, $\boldsymbol{r_{CM}}$, by using sensor data in an online estimation method. Then, the process was followed by a balancing method according to three movable masses. In their results, the reduction of the offset vector achieved the order of 0.1 mm corresponding to a period of 60 seconds for each oscillation.

In this paper, two schemes were adopted to reduce the disturbances in a small air-bearing spherical attitude simulator. The first one consists of the automatic mass balancing of the attitude simulator where Euler parameters and least-square batch estimation method were combined together to get a first estimation of the offset vector (or torque gravity vector) according to the parameters of a small satellite 1U-class CubeSat platform. At this stage, only static unbalance was considered as the main source of perturbation, and the disturbances coming from moving parts, deformation, and vibration of structures were neglected because of their order of magnitude. In practice, the later disturbances have a big impact on larger structures [6], [17], while for a CubeSat platform, those disturbances can be neglected during the batch estimation scheme. The second scheme deals with parameter uncertainty and external perturbations in the system. This scheme includes augmenting an adaptive controller to a feedback control law to improve robustness and attain the desired performance in an online compensation. Simulation and analysis of the balancing method along with an adaptive control architecture, present the feasibility for further implementation.

Existing results on control of satellites, testbeds, and attitude simulator systems were proposed, for example, on feedback [18], proportional-derivative [19], back-stepping [20], sliding-mode [21], optimal [22], adaptive [23], and model predictive control [24], while some authors exploit neural networks within adaptive control approach for uncertainty systems [25]. However, the robustness aspects provided by control laws based on proportional-derivative, feedback-linearization, back-stepping, and optimal frameworks are usually minimal or restricted because of the conservativeness in the design. Other controllers, such as the sliding-mode control, offer great robustness, but in practice, the chattering phenomenon makes it difficult to implement. Model predictive control and neural networks provide acceptable results for robust controllers except of the drawback of high computational cost.

In the literature, different approaches using adaptive techniques have been proposed to improve control performance and increase robustness against parameter uncertainty, external perturbation, and actuator/sensor faults. Arabi and Tansel. generalized a set-theoretic model reference adaptive control framework to enforce a user-define performance bounds, which gives the user the flexibility of control performance in transient and steady-state response inside a close loop system [26], [27]. In their research, Dizhi trained recurrent neural networks to improve system accuracy by transforming an estimated neural network model into a generalized nonlinear system without sensor faults terms [28].

For our attitude simulator, the exchange moments are induced by three reaction wheels (RW) to deliver control inputs. At first, an error feedback control law was designed to

introduce a proportional-derivative nominal control law in a closed-loop trajectory for tracking error dynamics. Since the inertia of the attitude simulator is unknown, the error feedback control law cannot guarantee satisfactory performance of the tracking trajectory. In consequence, a modular control architecture was proposed, where the proportional-derivative control law can be augmented with an alternative control technique, in this case, with a model reference adaptive control (MRAC) law, to improve robustness and attain satisfactory performance.

In this scenario, the present paper proposes the following contributions:

(i) Reduced dynamics equations of motion with Euler parameters representation
(ii) Automatic mass balancing system for attitude simulator platform
(iii) Comparison and simulation response for the estimated offset vector at each testing time
(iv) User-defined error performance for tracking desired Euler angle command for CubeSat attitude simulator
(v) Improved controller performance by MRAC with input error modification to counteract parametric uncertainty and unknown external disturbance

This paper is organized as follows. In section II, the dynamic model and the automatic balancing system are presented. In Section III, an overview and a formalized MRAC is presented. Section IV presents the proposed control law with input error modification design. In section V, a description of the spherical attitude simulator parameters, along with the simulation setup, is presented. In section VI, numerical simulation results are discussed. Finally, in section VII, the conclusion and future works are presented.

II. SYSTEM MODELING

In this section, the attitude motion of a small spacecraft is described along with the nonlinear model for an attitude simulator system. Next, the least-square batch estimation method and automatic mass balancing system for the attitude testbed simulator are presented.

A. SATELLITE ATTITUDE NONLINEAR MODEL

In this part of the section, the model of the satellite dynamics is derived from the Newton-Euler formulation (1), where $\boldsymbol{\omega}_{ib}^{b}$ be the angular velocity of the body frame with respect to the inertial frame, expressed in the body frame. J be the moment of inertia of the satellite, $\boldsymbol{h} = J\boldsymbol{\omega}_{ib}^{b}$ be the angular momentum of the body and $\boldsymbol{M}_{ext}^{b}$ be the external moment acting on the body composed of both internal and external torques [29]. The internal torques (such as the micro-vibrations caused by junctions, rotors, thermal deformations, etc.) can be neglected and considered minimal in comparison to the external torques [30], [31].

$$\left(\frac{d\boldsymbol{h}}{dt}\right) = J\dot{\boldsymbol{\omega}}_{ib}^{b} = -\boldsymbol{\omega}_{ib}^{b} \times J\boldsymbol{\omega}_{ib}^{b} + \boldsymbol{M}_{ext} \tag{1}$$

Considering a small satellite, the group of external torques $\boldsymbol{M}_{ext}^{b}$ acting on the body, (2), can be divided into two groups. One for the control input torque and the second one for the disturbance torque $\boldsymbol{\tau}_{d}^{b}$. In our design, the former one is composed of a set of reaction wheels applying momentum exchange to the body, $\boldsymbol{\tau}_{rw}^{b}$. The latter one is normally composed of a gravity gradient $\boldsymbol{\tau}_{gg}^{b}$, solar radiation $\boldsymbol{\tau}_{sr}^{b}$, aerodynamic drag $\boldsymbol{\tau}_{ad}^{b}$, and parasite magnetic dipole torque $\boldsymbol{\tau}_{pm}^{b}$, (3).

$$\boldsymbol{M}_{ext} = \boldsymbol{\tau}_{d}^{b} + \boldsymbol{\tau}_{rw}^{b} \tag{2}$$

$$\boldsymbol{\tau}_{d}^{b} = \boldsymbol{\tau}_{gg}^{b} + \boldsymbol{\tau}_{sr}^{b} + \boldsymbol{\tau}_{ad}^{b} + \boldsymbol{\tau}_{pm}^{b} \tag{3}$$

The nonlinear kinematics equations of motion can be represented by Euler parameters (4) where η be the real part of the quaternion, $\boldsymbol{\varepsilon}$ be the vector part, $S(\boldsymbol{\varepsilon})$ be the skew symmetric matrix of $\boldsymbol{\varepsilon}$, and $\boldsymbol{\omega}_{ob}^{b}$ be the angular velocity of the body frame with respect to the orbital frame, expressed in the body frame [30], [32], [33].

$$\dot{\boldsymbol{q}} = \begin{bmatrix} \dot{\eta} \\ \dot{\boldsymbol{\varepsilon}} \end{bmatrix} = \frac{1}{2}\begin{bmatrix} -\boldsymbol{\varepsilon}\ T \\ \eta + S(\boldsymbol{\varepsilon}) \end{bmatrix} \boldsymbol{\omega}_{ob}^{b} \tag{4}$$

B. ATTITUDE SIMULATOR NONLINEAR MODEL

Similar to the general equations of motion for an orbiting rigid-body spacecraft (1) (4), the dynamic equations of motion of an attitude simulator, represented in the body coordinate frame, can be written considering a gravity vector torque acting on the body (5). Let J_s be the moment of inertia of the attitude simulator system, $\boldsymbol{\omega}$ be the absolute angular velocity of the body, $\boldsymbol{h}_s = J_s\boldsymbol{\omega}$ be the angular momentum of the overall system, $\boldsymbol{M}_{ext}$ be the group of external moment acting on the system (6). Where $\boldsymbol{\tau}_c$ be the control input torque, $\boldsymbol{\tau}_d$ be the external disturbance torque, M_s be the total mass of the system, $\boldsymbol{g}$ be the acceleration of gravity vector acting on the body at ground testing level, and $\boldsymbol{r}_{CM}$ be defined as the offset vector between the CM and the CR, expressed in the body coordinate frame. (Note that, for simplicity, the superscripts in the following equations of motion are omitted since it is assumed that all of them are represented in the body coordinate frame unless it is told differently).

$$\left(\frac{d\boldsymbol{h}_s}{dt}\right) = J_s\dot{\boldsymbol{\omega}} = -\boldsymbol{\omega} \times (J\boldsymbol{\omega}) + \boldsymbol{M}_{ext} \tag{5}$$

$$\boldsymbol{M}_{ext} = \boldsymbol{\tau}_c + \boldsymbol{\tau}_d + \boldsymbol{r}_{CM} \times M_s\boldsymbol{g} \tag{6}$$

In this work, we adopted the Euler parameter representation to describe the equations of motion, hence, let η_s be the real part of the quaternion, $\boldsymbol{\varepsilon}_s$ be the vector part, and $S(\boldsymbol{\varepsilon}_s)$ be the skew-symmetric matrix of $\boldsymbol{\varepsilon}_s$. The nonlinear kinematics equation of motion of the attitude simulator can be written as:

$$\dot{\boldsymbol{q}} = \begin{bmatrix} \dot{\eta}_s \\ \dot{\boldsymbol{\varepsilon}}_s \end{bmatrix} = \frac{1}{2}\begin{bmatrix} -\boldsymbol{\varepsilon}_s^{T} \\ \eta_s + S(\boldsymbol{\varepsilon}_s) \end{bmatrix} \omega \tag{7}$$

It is worth mentioning that the gravitational torque generated by the vector $\boldsymbol{r}_{CM}$ be the main disturbance which be estimated by the least squares batch method. Other disturbances are not considered at this stage because of their order of magnitude $\boldsymbol{\tau}_d \approx \boldsymbol{0}$. In order to perform the parameter

estimation method, no control input torque is assumed ($\boldsymbol{\tau_c} = 0$) according to the pendulum-like motion produced by the vector offset $\boldsymbol{r_{CM}}$.

C. REDUCED EQUATION OF MOTION

To reduce computational complexity, the dynamic equations of motion of the attitude simulator can be greatly simplified by considering that the products of the inertia matrix J_s and the angular rates of the body ω are small enough compared to the other terms [33]. Let $\begin{bmatrix} r_{CM_x} & r_{CM_y} & r_{CM_z} \end{bmatrix}^T$ be the elements of the offset vector $\boldsymbol{r_{CM}}$, $diag\,(J_s) = \begin{bmatrix} J_{xx} & J_{yy} & J_{zz} \end{bmatrix}$ be the principal diagonal of matrix corresponding to the moment of inertia J_s, M_s be the system mass, and $\begin{bmatrix} q_0 & q_1 & q_2 & q_3 \end{bmatrix}^T$ be the elements of the quaternion $\boldsymbol{q_s}$ representing the rotation of the simulator in the body coordinate frame.

Then, by applying the small angle assumption and transforming (5) into the Euler parameter representation, the dynamic equations of motion can be rewritten as:

$$\dot{\boldsymbol{\omega}} = \begin{bmatrix} \frac{M_s g}{J_{xx}} \left(-r_{CM_y} + r_{CM_z}\left(4q_2q_3 - 2q_1\right)\right) \\ \frac{M_s g}{J_{yy}} \left(r_{CM_x} + r_{CM_z}\left(-2q_2 - 4q_1q_3\right)\right) \\ \frac{M_s g}{J_{zz}} \left(-r_{CM_x}\left(4q_2q_3 - 2q_1\right) - r_{CM_y}\left(-2q_2 - 4q_1q_3\right)\right) \end{bmatrix} \tag{8}$$

D. LEAST SQUARE BATCH ESTIMATION

Before performing the estimation of the vector offset, first, we calculated the increment of the angular rate $\Delta\boldsymbol{\omega}$ by performing simple integration over the angular rate of the simulator (8) within a few periods of the pendulum-like motion ($\approx 3T$) while assuming small time-step Δt (9). Assuming D be a constant matrix for a given time step, let M_D be a skew-symmetric matrix in the dynamical system with matrix elements (M_{32}, M_{13}, M_{21}) (10) composed by the current time-step (t_2) and previous time-step (t_1) of Euler parameters representing the motion of the attitude simulator (11).

$$\Delta\boldsymbol{\omega} = \boldsymbol{\omega_{t2}} - \boldsymbol{\omega_{t1}} = \frac{M_s \boldsymbol{g} \Delta t}{2} J^{-1} M_D \begin{bmatrix} r_x \\ r_y \\ r_z \end{bmatrix} = (D)\,(\boldsymbol{r_{CM}}) \tag{9}$$

$$M_D = \begin{bmatrix} 0 & -M_{21} & M_{13} \\ M_{21} & 0 & -M_{32} \\ -M_{13} & M_{32} & 0 \end{bmatrix} \tag{10}$$

$$\begin{aligned} M_{13} &= \left(4q_{2_{t2}}q_{3_{t2}} - 2q_{1_{t2}}\right) + \left(4q_{2_{t1}}q_{3_{t1}} - 2q_{1_{t1}}\right) \\ M_{21} &= 2 \\ M_{32} &= \left(4q_{1_{t2}}q_{3_{t2}} + 2q_{2_{t2}}\right) + \left(4q_{1_{t1}}q_{3_{t1}} + 2q_{2_{t1}}\right) \end{aligned} \tag{11}$$

In order to estimate the offset vector $\tilde{\boldsymbol{r}}_{\boldsymbol{CM}}$, we adopted the least square batch estimation method (12). It can be done by computing the inverse of matrix D times the increment of the absolute angular rate $\Delta\omega$.

$$\tilde{\boldsymbol{r}}_{\boldsymbol{CM}} = \left(D^{-1}\right)(\Delta\boldsymbol{\omega}) \tag{12}$$

Remark 1: we can get a first estimation of the pendulum-like motion period $\tilde{T}$ by measuring the window-time length between peak values in the states of the attitude motion of the system (Euler angles/angular rates).

E. AUTOMATIC MASS BALANCING SYSTEM

To perform the automatic mass balancing system, let $\boldsymbol{r_{m_i}}$ be the travelling distance of the moveable mass m_i located along each principal axis of the attitude simulator ($i = 1, 2, 3$), and M_s defined as the total mas of the system (13). Then, by letting the movable masses travel along the attitude simulator's principal axis at a distance $\Delta\boldsymbol{r_m}$ (14), the offset vector $\boldsymbol{r_{CM}}$ can be modified and reduced each iteration time [16].

$$\boldsymbol{r_{CM}} = \frac{1}{M_s} \sum_{i=1}^{3} m_i \boldsymbol{r_{m_i}} \tag{13}$$

where the travelled distance $\Delta\boldsymbol{r_m}$ be represented by the relationship between the elements of the current offset vector $\boldsymbol{r_{CM}}$ and each individual moveable mass m_i, as follows:

$$\Delta\boldsymbol{r_m} = -M_s \begin{bmatrix} r_{CM_x}/m_1 \\ r_{CM_y}/m_2 \\ r_{CM_z}/m_3 \end{bmatrix} \tag{14}$$

Remark 2: the vector offset $\boldsymbol{r_{CM}}$ can be especially hard to reduce when the inertia of the body is particularly small. This will cause the need for a fine displacement by the moving masses. Then, in order to get a satisfactory reduction of the gravity disturbance torque generated by the unbalanced system, especial care must be addressed in the design of the displacement of the moving masses.

After performing and identifying all variables in the system, the least square batch approximation method can be applied as many times as required. While some authors reported that no significant increment in the performance can be noticed after three iterations [16], in this paper, we assumed that the system is acceptably balanced after a pendulum period over 100 seconds and an amplitude of the angular motion reduced below 0.01 degree for each Euler angle.

In a system where static unbalance is only considered, the gravitational torque varies according to the attitude motion of the simulator. This motion can be represented by a set of Euler angles. While these angles are inherently linked together because of the dynamic equations of motion, we can calculate the amplitude and frequency of oscillations of the pendulum-like motion to evaluate the effectiveness of the automatic balancing method. Let J_{xx} be any of the components of the principal diagonal of the inertia matrix J_s, g defined as the acceleration of gravity at ground testing level, and $\|\boldsymbol{r_{CM}}\|_2$ be the Euclidian norm of the offset vector $\boldsymbol{r_{CM}}$. The period of a simple pendulum in free motion can be calculated as [34]:

$$T = \frac{2\pi}{\sqrt{\frac{M_s g}{J_{xx}} \|\boldsymbol{r_{CM}}\|_2}} \tag{15}$$

TABLE 1. Math notations.

Notation	Description	Notation	Description
ϕ, θ, ψ	Euler angles	$\omega_1, \omega_2, \omega_3$	Angular rates
J_s	Moment of inertia of the simulator	J_{11}, J_{22}, J_{33}	Simulator axis moment of inertia
$\boldsymbol{x_p}(t) \in \mathbb{R}^{6\times1}$	Measurable system state vector	$A_p \in \mathbb{R}^{6\times6}$	System state matrix
$W_p(t) \in \mathbb{R}^{6\times3}$	Bounded unknown weight matrix	$B_p \in \mathbb{R}^{6\times3}$	Control input matrix
$\boldsymbol{c}(t) \in \mathbb{R}^{3\times1}$	Piecewise command	$\boldsymbol{x_c}(t) \in \mathbb{R}^{3\times1}$	Integral state
$\Lambda \in \mathbb{R}^{3\times3}$	Unknown control effectiveness matrix	δ_p: $\overline{\mathbb{R}}^+(\mathbb{R}^{3\times1})$	System uncertainty
$E_p \in \mathbb{R}^{3\times6}$	Matrix subset following selector	σ_p: $\mathbb{R}^{6\times1}$	Known basis function
$\boldsymbol{x}(t) \in \mathbb{R}^{9\times1}$	Augmented state vector	$\boldsymbol{u_n}(t) \in \mathbb{R}^{3\times1}$	Nominal control law
$A \in \mathbb{R}^{9\times9}$	Augmented system state matrix	$\boldsymbol{u_a}(t) \in \mathbb{R}^{3\times1}$	Adaptive control law
$B \in \mathbb{R}^{9\times3}$	Augmented control input matrix	$W(t) \in \mathbb{R}^{15\times3}$	Unknown weight matrix
$A_r \in \mathbb{R}^{9\times9}$	Adaptive system state matrix	$\sigma \in \mathbb{R}^{15\times3}$	Known basis function
$B_r \in \mathbb{R}^{9\times3}$	Adaptive control input matrix	$K \in \mathbb{R}^{3\times9}$	Nominal feedback gain
$\boldsymbol{x_r} \in \mathbb{R}^{9\times3}$	Reference state vector	$\gamma \in \mathbb{R}^+$	Learning rate
$\boldsymbol{u}(t) \in \mathbb{R}^{3\times1}$	Feedback control law	$\widehat{W}(t) \in \mathbb{R}^{15\times3}$	Estimate $W(t)$
$\varphi_d(\|\boldsymbol{e}(t)\|_p)$	Error-dependent learning rate	$\widetilde{W}(t) \in \mathbb{R}^{15\times3}$	Estimate of error $W(t)$
$(\cdot)^T$	Transpose operator	$\boldsymbol{e}(t) \in \mathbb{R}^{9\times1}$	System error
$(\cdot)^{-1}$	Inverse operator	P: $\mathbb{R}^+(\mathbb{R}^{9\times9})$	A solution of Lyapunov equation
$det(\cdot)$	Determinant operator	R: $\mathbb{R}^+(\mathbb{R}^{9\times9})$	Symmetric matrix
$I^n \in \mathbb{R}^{n\times n}$	Identity matrix $n \times n$	$0^{n\times m} \in \mathbb{R}^{n\times m}$	Null matrix $n \times m$
$\|\cdot\|_2$	Euclidian norm	$\|\boldsymbol{x}\|_A \triangleq \sqrt{\boldsymbol{x}^T A \boldsymbol{x}}$	Weighted Euclidian norm of $\boldsymbol{x}$
$tr(\cdot)$	Trace operator	$\|A\|_2 \triangleq \sqrt{\lambda_{max}(A^T A)}$	Induced 2-norm of the matrix A
$\lambda_{min}(A)$	Minimum eigenvalue of matrix A	$\underline{\boldsymbol{x}}$	Lower bound of bounded $\boldsymbol{x}(t)$
$\lambda_{max}(A)$	Maximum eigenvalue of matrix A	$\overline{\boldsymbol{x}}$	Upper bound of bounded $\boldsymbol{x}(t)$

Finally, to validate the automatic balancing mass system performance, the calculated period (15) can be compared to the one estimated with the pendulum-like motion in remark 1.

III. MODEL REFERENCE ADAPTIVE CONTROL DESIGN

In this section, an uncertain dynamical system representing an unbalanced attitude simulator system with unknown perturbation is addressed, where the tracking performance can be guaranteed according to a leakage modification in the MRAC [26], [27], [49] and the proposed input error modification for a dynamical system such as the attitude simulator.

A. MODEL REFERENCE ADAPTIVE CONTROL

Let $\boldsymbol{x_p}(\mathbf{t})$ be the measurable state vector of an uncertainty system, A_p, B_p be the known system matrix, and control input matrix, respectively, with both matrices controllable, $\boldsymbol{u}(t)$ be the control input. Λ be the unknown control effectiveness matrix, and δ_p be the system uncertainty. Then, a dynamical system with parameter uncertainty and unknown external perturbation can be written in the following form:

$$\begin{aligned} \dot{\boldsymbol{x_p}}(t) &= A_p \boldsymbol{x_p}(t) + B_p \Lambda u(t) + B_p \delta_p\left(t,\ \boldsymbol{x_p}(t)\right), \\ \boldsymbol{x_p}(0) &= \boldsymbol{x_{p0}} \end{aligned} \tag{16}$$

Assumption 1: consider a given bounded unknown weight matrix W_p, where $\|W_p\|_2 \leq w_p$ for $t \geq 0$, has a bounded time rate of change $\|\dot{W}_p\|_2 \leq \dot{w}_p$ for $t \geq 0$, Let $\sigma_p\left(\boldsymbol{x_p}\right) = [\sigma_{p1}\left(\boldsymbol{x_p}\right), \sigma_{p2}\left(\boldsymbol{x_p}\right), , \ldots, \sigma_{ps}\left(\boldsymbol{x_p}\right)]^T$ be a known basis function that includes local Lipschitz elements. Then, the system uncertainty δ_p at (16) can be parameterized as [35], [36], and [37]:

$$\delta_p\left(t,\ \boldsymbol{x_p}\right) = W_P^T(t)\sigma_p\left(\boldsymbol{x_p}\right) \tag{17}$$

By definition, the system uncertainty $\delta_p(t, \boldsymbol{x_p})$ is able to size time-varying changes as, for example, the parameter uncertainty of a non-rigid spacecraft inertia. Furthermore, by letting some of the basis function elements be constant (e.g. $\sigma_{p1}(\boldsymbol{x_p}) = cte$), the uncertainty of the system $\delta_p(t, \boldsymbol{x_p})$ is able to capture external time-varying disturbances such as the four types mentioned for the attitude simulator system.

In order to include the command following into the system, let the state vector be augmented with an integral state $\boldsymbol{x_c}(\mathbf{t})$. Let E_p be a matrix subset following selector, and $\boldsymbol{c}(t)$ be a piecewise command; hence, the augmented vector can be defined as $\boldsymbol{x}(t) \triangleq \left[\boldsymbol{x_p^T}(t)\ \boldsymbol{x_c^T}(t)\right]^T$ where the integral term $\boldsymbol{x_c}(\mathbf{t})$ satisfies (18).

$$\begin{aligned} \dot{\boldsymbol{x_c}}(t) &= E_p \boldsymbol{x_p}(t) - \boldsymbol{c}(t), \\ \boldsymbol{x_c}(0) &= \boldsymbol{x_{c0}} \end{aligned} \tag{18}$$

In order to acquire the desired command following characteristics taken by the reference model (19), let $A_r \triangleq A - BK$ be Hurwitz to get bounded reference state vector $\boldsymbol{x_r}$, $B_r \triangleq \left[0^{3\times6}\ -I^{3\times3}\right]^T$ be the adaptive control input matrix and $B_r \boldsymbol{c}(t)$ be the nominal control signal. Where A and B be the

state matrices of an augmented system described at (20).

$$\dot{\boldsymbol{x}}_{\boldsymbol{r}}(t) = A_r \boldsymbol{x}_{\boldsymbol{r}}(t) + B_r \boldsymbol{c}(t),$$
$$\boldsymbol{x}_{\boldsymbol{r}}(0) = \boldsymbol{x}_{\boldsymbol{r0}},\ t \geq 0 \tag{19}$$
$$A \triangleq \begin{bmatrix} A_p & 0^{6\times 3} \\ E_p & 0^{3\times 3} \end{bmatrix},\ B \triangleq \begin{bmatrix} B_p^T & 0^{3\times 3} \end{bmatrix} \tag{20}$$

Then, by considering (16), (17), (18), and (19), the augmented system can be written as:

$$\boldsymbol{x}(t) = A\boldsymbol{x}(t) + B\Lambda \boldsymbol{u}(t) + BW_P^T(t)\sigma_p\left(\boldsymbol{x_p}(t)\right) + B_r \boldsymbol{c}(t),$$
$$\boldsymbol{x}(0) = \boldsymbol{x_0},\ t \geq 0 \tag{21}$$

To formulate the feedback control law (22), let $\boldsymbol{u_a}(t)$ be the adaptive control law (24), and $\boldsymbol{u_n}(t)$ be the nominal control law (23).

$$\boldsymbol{u}(t) = \boldsymbol{u_n}(t) + \boldsymbol{u_a}(t),\ t \geq 0 \tag{22}$$
$$\boldsymbol{u_n}(t) = -K\boldsymbol{x}(t),\ t \geq 0 \tag{23}$$

Assuming an unknown weight matrix be $W(t) \triangleq [\Lambda^{-1}W_p^T(t)\ \left(\Lambda^{-1} - I^{3\times 3}\right)K]^T$, a known basis function be $\sigma(\boldsymbol{x}(t)) \triangleq \left[\sigma_p^T(\boldsymbol{x}(t))\ \boldsymbol{x}^T(t)\right]^T$, and $\hat{W}(t)$ be the estimate of $W(t)$ for $t \geq 0$ satisfying the update law (30), the adaptive control law can be written as:

$$\boldsymbol{u_a}(t) = -\hat{W}^T(t)\sigma\left(\boldsymbol{x}(t)\right),\ t \geq 0 \tag{24}$$

Let $\boldsymbol{x_r}(t)$ be the reference state vector which satisfies the uncertain dynamical system (25) obtained by combining (19), (21), and (22).

$$\boldsymbol{x}(t) = A_r \boldsymbol{x_r}(t) + B_r \boldsymbol{c}(t) + B\Lambda\left[\boldsymbol{u_a}(t) + W^T(t)\sigma\left(\boldsymbol{x}(t)\right)\right],$$
$$\boldsymbol{x}(0) = \boldsymbol{x_0},\ t \geq 0 \tag{25}$$

Let $e(t)$ be defined as the system error, and $\tilde{W}(t)$ be defined as the weight estimate error, where the system error dynamics (28) can be obtained by combining (19), (24), and (25).

$$\boldsymbol{e}(t) \triangleq \boldsymbol{x}(t) - \boldsymbol{x_r}(t),\ t \geq 0 \tag{26}$$
$$\tilde{W}(t) \triangleq W(t) - W(t),\ t \geq 0 \tag{27}$$
$$\dot{\boldsymbol{e}}(t) = A_r \boldsymbol{e}(t) - B\Lambda \tilde{W}^T(t)\sigma\left(\boldsymbol{x}(t)\right),$$
$$\boldsymbol{e}(0) = \boldsymbol{e_0} \triangleq \boldsymbol{x_0} - \boldsymbol{x_{r0}},\ t \geq 0 \tag{28}$$

To define the update law, let R be a symmetric matrix (29), and P be a solution of the Lyapunov equation given by:

$$0 = A_r^T P + PA_r + R \tag{29}$$

Remark 3: For a standard model reference adaptive controller, by considering a learning rate of adaptation gain γ, the update law (30) can be derived by choosing the Lyapunov function candidate as in (31) with time derivative (32) for a close loop system trajectory (see remark 2.2 and the derivative of the parameter adjustment in [23], and [26] respectively).

$$\dot{\hat{W}}(t) = \gamma\sigma\left(x(t)\right)\boldsymbol{e}^T(t)PB$$
$$\hat{W}(0) = \hat{W}_0,\ t \geq 0 \tag{30}$$

$$V\left(\boldsymbol{e}, \tilde{W}\right) = \boldsymbol{e}^T P \boldsymbol{e} + \gamma^{-1}\, tr\left[\left(\tilde{W}\Lambda^{1/2}\right)^T\left(\tilde{W}\Lambda^{1/2}\right)\right] \tag{31}$$

$$\dot{V}\left(\boldsymbol{e}, \tilde{W}\right) = -\|\boldsymbol{e}(t)\|_2^2 - 2\gamma^{-1}\, tr\,\Lambda\tilde{W}^T(t) * \left(\gamma\sigma\left(\boldsymbol{x}(t)\right)\boldsymbol{e}^T(t)PB - \dot{\hat{W}}\,(t)\right) \tag{32}$$

Remark 4: In adaptive control, one feature of interest is to reduce or eliminate the conservativeness of the design. While for a standard model reference adaptive controller, this conservativeness is high because of the upper and lower bounds on the unknown gains, in practice, it is not possible to adopt an upper bound in the control signal. In consequence, in this paper an adaptive controller with barrier Lyapunov function with leakage modification is adopted to acquire user-defined error performance.

To stablish the update law, let $\varphi_d(\|z\|_p)$ be defined as a generalized restricted barrier Lyapunov function on the set $D_\epsilon \triangleq \{\|z\|_H : \|z\|_H \in [0, \epsilon)\}$ where ϵ be a-priori user defined constant (see the definition of restricted potential functions in [27], [38], [39], [40], [41], [42], and [43]).

The update law in (30) can be augmented using the defined restricted potential function resulting in (33), where $\varphi_d\left(\|\boldsymbol{e}(t)\|_p\right)$ be the error depending learning rate.

$$\dot{\hat{W}}(t) = \gamma\varphi_d\left(\|\boldsymbol{e}(t)\|_p\right)\boldsymbol{e}^T(t)PB$$
$$\hat{W}(0) = \hat{W}_0,\ t \geq 0 \tag{33}$$

Then, considering the system error dynamics defined in (28), and introducing a leakage term κ [26], [49], the weight estimation error dynamics be given as:

$$\dot{\tilde{W}}(t) = \gamma\left(\varphi_d(\|\boldsymbol{e}(t)\|_p)\boldsymbol{e}^T(t)PB - (\kappa\hat{W}^T(t))^T\right),$$
$$\hat{W}(0) = \hat{W}_0,\ t \geq 0 \tag{34}$$

Next, from a theoretical point of view, the error dynamics can be strictly bounded by a user-defined given system error (user-defined worst-case performance) ϵ, (35), by applying the barrier Lyapunov function, (see *Lemma 1* in [40], [42]).

$$\|\boldsymbol{e}(t)\|_p < \epsilon,\ t \geq 0 \tag{35}$$

To design the feedback control law (22) with the user-defined system error performance ϵ, first, let the known basis function $\sigma(\boldsymbol{x})$ be restricted by an upper bound υ, $\|\sigma(\boldsymbol{x})\|_2 \leq \overline{\sigma} + \upsilon\|\boldsymbol{x}\|_2$. Hence, the new feedback control law of the system can be computed as in (36) (For reference, see theorem 3.2 at [27]).

$$\|\boldsymbol{u}(t)\|_2 \leq \|-K\boldsymbol{x}(t)\|_2 + \left\|-\hat{W}^T(t)\sigma\left(\boldsymbol{x}(t)\right)\right\|_2$$
$$\|\boldsymbol{u}(t)\|_2 \leq \|K\|_2\|\boldsymbol{x}(t)\|_2 + \hat{W}_{max}\left(\overline{\sigma} + \upsilon\|\boldsymbol{x}(t)\|_2\right)$$
$$\|\boldsymbol{u}(t)\|_2 \leq \left(\|K\|_2 + \hat{W}_{max}\upsilon\right)\left(\|\boldsymbol{e}(t)\|_2 + \bar{\boldsymbol{x}}_{\boldsymbol{r}}\right) + \hat{W}_{max}\overline{\sigma} \tag{36}$$

As the worst-case performance given at (35) depends only on the user-defined system error performance ϵ, this parameter can be designed in the a-priori stage, giving as a result a

guaranteed system performance written as in (37), and upper bounded feedback control law as in (38).

$$\|\boldsymbol{e}(t)\|_2 < \frac{\epsilon}{\sqrt{\lambda_{min}(P)}},\ t\geq 0 \tag{37}$$

$$\|\boldsymbol{u}(t)\|_2 \leq \left(\|K\|_2 + \hat{W}_{max}\upsilon\right)\left(\frac{\epsilon}{\sqrt{\lambda_{min}(P)}} + \overline{\boldsymbol{x_r}}\right) + \hat{W}_{max}\overline{\sigma},\ \ t\geq 0 \tag{38}$$

The stability of the modified MRAC architecture can be proven by considering the dynamical system (16), subject to assumption 1, along with the reference model given at (19), the feedback control law in (22), the nominal control law (23), the adaptive control law (24), and the update law (34) derived by choosing the Lyapunov function candidate at (39), and Lyapunov derivative at (40) [26], [27], where $\alpha \triangleq \frac{\lambda_{min}(R)}{\lambda_{max}(P)}$, $d \triangleq 2\gamma^{-1}\tilde{w}\dot{w}\|\Lambda\|_p$, $\mu = \frac{1}{2}\alpha\gamma^{-1} * \tilde{w}^2\|\Lambda\|_2 + d$, $\tilde{w} = \hat{W}_{max} + w$, $\|\mathrm{W}\|_F \leq w$, $\left\|\dot{\mathrm{W}}\right\|_F \dot{\leq} w$. getting $\dot{V}\left(\boldsymbol{e}(t), \hat{W}(t)\right)$ upper bounded and the system error satisfying the strict user-defined boundedness ϵ [40], [42].

$$V\left(\boldsymbol{e}(t), \tilde{W}(t)\right) = \varphi\left(\|\boldsymbol{e}(t)\|_p\right) + \gamma^{-1}\,\mathrm{tr}\left[\left(\tilde{W}\Lambda^{1/2}\right)^T\left(\tilde{W}\Lambda^{1/2}\right)\right] \tag{39}$$

$$\dot{V}\left(\boldsymbol{e}(t), \tilde{W}(t)\right) \leq = -\frac{1}{2}\alpha V\left((t), \tilde{W}(t)\right) + \mu \tag{40}$$

Note that, in this paper, the system-error learning rate $\gamma\,(\boldsymbol{e})$ is adopted to achieve a-priori, user-defined performance guarantees, while a leakage term κ is added into the parameter adjustment mechanism (34).

IV. CONTROL INPUT DESIGN FOR THE SPHERICAL ATTITUDE SIMULATOR

A. NOMINAL CONTROL INPUT DESIGN

In this part of the section, a nominal control design is introduced where a traditional PD feedback controller is implemented by considering the dynamics of a rigid-body spacecraft. Let x_{en} be the nominal error state (41), $\boldsymbol{q_e} = \tilde{\boldsymbol{q}} = [\tilde{\eta}\tilde{\boldsymbol{\varepsilon}}]^T$ be the quaternion error feedback, $\boldsymbol{\omega_e}$ be the body-rate feedback, $[k,\ d]$ be real nonnegative gains, and a nominal torque input $\boldsymbol{u_n}$ governed by (42). $s\,(\boldsymbol{\omega_e})\,J_s\boldsymbol{\omega_e}$ be a term usually used to counteract a possible gyroscopic coupling torque but omitted in case of slow rotational maneuvers.

$$\boldsymbol{x_{en}} = \left[\boldsymbol{q_e}\boldsymbol{\omega_e}\right]^T \tag{41}$$

$$\boldsymbol{u_n} = -s\,(\boldsymbol{\omega_e})\,J_s\boldsymbol{\omega_e} - k\boldsymbol{q_e} - d\boldsymbol{\omega_e} \tag{42}$$

The nominal controller u_n in (42) is about minimizing the error between the desired and current attitude of the small satellite attitude simulator where the real part of the quaternion error tends to be one ($\tilde{\eta} \to \pm 1$), and the vector part tends to zero ($\tilde{\boldsymbol{\varepsilon}} \to 0$), while the body-rate feedback error goes to zero ($\tilde{\boldsymbol{\omega}} \to 0$).

B. MODIFIED ADAPTIVE CONTROL INPUT DESIGN

As written in (24), the adaptive control law $\boldsymbol{u_a}(t)$ is bounded by a known basis function $\sigma\,(\boldsymbol{x}(t))$, and an estimated unknown weight matrix $\hat{W}$, in which case in order to counteract conservativeness, the later one is also bounded by a-priori user-defined constant (also known as system error performance) ϵ (35). Then, as long as the user-defined boundary is accomplished, the adaptive controller stability can be guaranteed.

While the adopted design of the adaptive control with leakage modification runs under specified boundaries with strict user-defined performance given by the system error performance ϵ, a satellite attitude simulator still demands high precision, along with high stability. Different aspects can cause the anomaly attitude stability in Fig. 8; one potential cause is that the adaptive law (30) implements system errors in the adjustment of the control parameter, usually requiring persistent excitation (external disturbances) and sufficiently large amplitude [44].

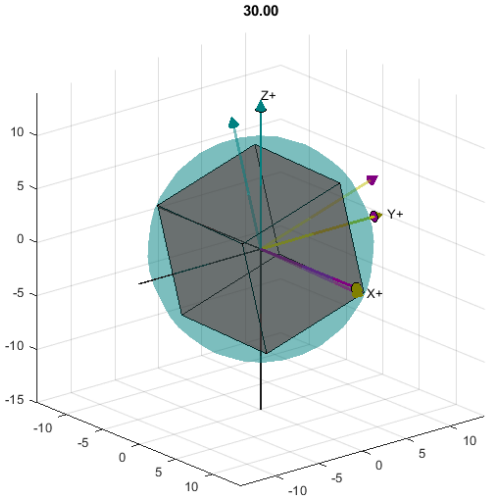

FIGURE 1. Spherical 1U-CubeSat attitude simulator platform.

Motivated by improving the attitude stability of the attitude simulator, a variation of the adaptive control law (24) is proposed in (43) where the controller is not just bounded by the system error performance ϵ, hence, the unknown weight matrix $W(t)$, but it be also bounded according to the nominal controller $\boldsymbol{u_n}(t)$ (23) which be previously designed with user-defined performance according to the set of model reference control specifications (42).

$$\boldsymbol{u_a}(t) = \begin{cases} \boldsymbol{u_n}, & \|\boldsymbol{u_a}(t)\|_2 \geq \|\boldsymbol{u_n}(t)\|_2 \\ \boldsymbol{u_a}, & otherwise \end{cases},\ t\geq 0 \tag{43}$$

Now, assuming that the proposed adaptive control law (43) be bounded by the nominal control law (42), the upper bound of the feedback control law (22) can be rewritten as:

$$\boldsymbol{u}(t) = \begin{cases} -2\|K\|_2\|\boldsymbol{x}(t)\|_2, & \|\boldsymbol{u_a}(t)\|_2 \geq \|\boldsymbol{u_n}(t)\|_2 \\ -K\boldsymbol{x}(t) - \hat{W}^T(t)\sigma\,(\boldsymbol{x}(t))\,, & otherwise, \end{cases} \quad t\geq 0 \tag{44}$$

Theorem 1: the system control input designed in (44) guarantees asymptotic stability for the attitude simulator dynamical system with parameter uncertainty and unknown disturbances given by (16) subject to assumption one such that the output states $\boldsymbol{x}(t)$ converge to the reference command $\boldsymbol{c}(t)$ in finite time. Furthermore, the reference model given in (19), along with the feedback control law (22), the nominal control law (42) augmented with the integral term according to (48), and the new adaptive control law (43), guarantee asymptotic stability while the nominal error (41), and system error (26), converge to zero in finite time.

Proof: the stability of the closed-loop system can be proven with general d and k matrices, where the feedback nominal gain is given by $K_{PD} = n_g \left[\, k \;\; d \,\right]$. Assuming that k^{-1} exists, n_g be a real nonnegative gain and $\tilde{\eta}$ belongs to the real part of the composed nominal error set of Euler parameters $\boldsymbol{x_{en}}$, we can choose a generalization of the Lyapunov function candidate [22], [45] given by:

$$V\left(\boldsymbol{x_{en}}\right) = \frac{1}{2}\boldsymbol{\omega}^T\left(n_g k\right)^{-1} J\boldsymbol{\omega} + 2\left(1\tilde{-}\eta\right) \tag{45}$$

With the Lyapunov time derivative given by:

$$\begin{aligned} V\left(\boldsymbol{x_{en}}\right) &= \frac{1}{2}\dot{\boldsymbol{\omega}}^T\left(n_g k\right)^{-1} J\boldsymbol{\omega} + \frac{1}{2}\boldsymbol{\omega}^T\left(n_g k\right)^{-1} \dot{J}\boldsymbol{\omega} - 2\dot{\tilde{\eta}} \\ \dot{V}\left(\boldsymbol{x_{en}}\right) &= \boldsymbol{\omega}^T\left(n_g k\right)^{-1} \dot{J}\boldsymbol{\omega} - 2\dot{\tilde{\eta}} \\ V\left(\boldsymbol{x_{en}}\right) &= -\boldsymbol{\omega}\, T\left(n_g k\right)^{-1}\left(n_g d\right)\boldsymbol{\omega} + (1-\mu)\left(n_g k\right)^{-1} \mathrm{s}\left(\boldsymbol{\omega}\right) J\boldsymbol{\omega} \end{aligned} \tag{46}$$

Assuming precise cancellation of the gyroscopic term $\mu = 1$, the derivative of V can be reduced to:

$$\dot{V}\left(\boldsymbol{x_{en}}\right) = -\boldsymbol{\omega}\, T\left(n_g k\right)^{-1}\left(n_g d\right)\boldsymbol{\omega} \tag{47}$$

In consequence, global stability can be guaranteed if $\left(n_g k\right)^{-1}\left(n_g d\right) > 0$. Where d be a positive real number.

Finally, the second term in (44) had been proven by the stability conditions for the adaptive control design (39), and (40).

Remark 5: in order to implement the integral term into the proposed control law, let the nominal control law (42) be augmented into the new nominal control law given at (49) according to the *PID* controller gains design in (48) whit time constant of integral control T_i [46]. Note that in the proposed model, the feedback reference model at (19) gets replaced by the error feedback reference model (50), where the nominal error $\boldsymbol{x_{en}}$ is augmented with the integral term $\boldsymbol{x_c}(t)$ into the reference error state $\boldsymbol{x_{er}}(t) = \left[\boldsymbol{x_{en}^T}(t)\;\boldsymbol{x_c^T}(t)\right]^T$. The asymptotic stability of the controller can be guaranteed as long as $\lim_{t\to\infty} \boldsymbol{x_{en}} = \left[0^{1\times 6}\right]^T$, $\lim_{t\to\infty} \boldsymbol{x_{er}} = \left[0^{1\times 9}\right]^T$.

$$k_p = k, \qquad k_i = k/T_i,\; k_d = d \tag{48}$$

$$\boldsymbol{u_{en}} = -K_{PID}\boldsymbol{x_{er}}, \tag{49}$$

$$\begin{aligned} K_{PID} &= \left[\, k \;\; d \;\; i \,\right] \\ \dot{\boldsymbol{x}}_{\boldsymbol{r}}(t) &= A\boldsymbol{x_r}(t) + B\boldsymbol{u_{en}}, \\ \boldsymbol{x_r}(0) &= \boldsymbol{x_{r0}},\; t \geq 0 \end{aligned} \tag{50}$$

V. TESTBED DESCRIPTION AND SIMULATION SETUP

A. SPHERICAL CLASS 1U-CUBESAT PLATFORM

In order to simulate the attitude motion of an orbiting small satellite (1U-class CubeSat platform) with uncertain inertia and unknown perturbations in the LEO, the orbital parameters and the attitude simulator parameters are presented in this part of the section.

Let $h = 500$ km be the orbit flight altitude in a circular orbit (eccentricity $=$ 0) around the Earth with orbit inclination $i = 97.4°$, and local ascending node time $10 : 30$ am. Assuming Earth radius $R_\oplus \approx 6378$ km, and Earth's mass $M_\oplus \approx 5.974 \times 10^{24}$kg, results in a circular orbital period of $T_{circular} \approx 94.62$ min, with a gravitational parameter $\mu \approx 398600\ \mathrm{km}^3/\mathrm{s}^2$, and an estimated satellite angular velocity of $\omega_o \approx 0.00110678$ rad/s (see [47], and [48] for orbital mechanics, and orbital dynamics equations of motion).

TABLE 2. CubeSat testbed platform parameters.

Symbol	Parameter	Value
h	Orbit Altitude	500 km
ω_o	Orbital angular velocity	≈ 0.00110678 rad/s
J_s	Principal diagonal of inertia matrix diag(J_S)	[4.26 4.26 4.26] $\times 10^{-3}$Kg.m^2
M	Total platform mass	2.56 Kg
m_i	Movable masses at each principal axis (i = 1,2,3)	0.1 Kg
$\dot{\boldsymbol{h}}_i$	RW exchange momentum at each axis (i = 1,2,3)	0.1 mN · m
$\boldsymbol{\Omega}_i$	RW nominal speed	3500 RPM
$\boldsymbol{r_{CM}}$	Gravity offset vector	$[-0.0095;\ 0.0712;\ -0.498]\times 10^{-5}$ m
$\boldsymbol{q_0}$	Initial attitude conditions	$[1,0,0,0]^{\mathrm{T}}$
$\boldsymbol{\omega_0}$		$[0,0,0]^{\mathrm{T}}$ rad/s
$\boldsymbol{u_0}$	Initial control input	$[0,0,0]^{\mathrm{T}}$ N · m

Assuming a rigid body CubeSat with uniform density in a 10 cm of size by side and 2.56 kg of weight, and acceleration of gravity at sea level $g_0 = 9.807\ \mathrm{m/s}^2$, let the principal diagonal of the moment of inertia matrix of the attitude simulator be given as $\mathrm{diag}\left(J_s\right) \approx [4.26,\ 4.26,\ 4.26] \times 10^{-3}\ \mathrm{kg.m}^2$ [50], [51], [52].

We let the actuator be chosen according to the requirements of the flight mission for the attitude control system. Hence, reaction wheels are considered well-suited to provide external torque to the spherical simulator platform. Hence, the main actuator of the active control input is a set of 3 RW, aligned with each principal axis of the testbed, able to deliver a maximum momentum exchange of 0.1 mN·m each second with nominal speed of 3500 RPM. To this end, the main parameters of the small satellite 1U-class CubeSat platform inside a spherical structure, Fig. 1, are listed in Table 2.

B. CONTROL PARAMETERS AND SIMULATION SETUP

To simulate the pendulum-like motion, let the gravity offset vector acting on the attitude testbed simulator (8) be given as $\boldsymbol{r_{CM}} = [\,-0.0095;\ 0.0712;\ -0.498\,] \times 10^{-5}$m, where according to the proposed scheme, this offset vector is the one to be estimated by the moving masses m_i in

the automatic balancing method. Other initial conditions, such as the attitude and angular rate, were set to the origin $\left(\boldsymbol{q} = [1, 0, 0, 0]^T, \boldsymbol{\omega} = [0, 0, 0]^T\right)$ (Note that, to apply the estimation method during this stage, no control input signals are acting on the system).

TABLE 3. Simulation and control parameters.

Symbol	Parameter	Value
$t_{0,1}^{offset}$	r_{CM} estimation time (T_0, T_1)	200 s
t_{2-6}^{offset}	r_{CM} estimation time (T_2) to (T_6)	300 s
Δt	Time-step	0.01 s
t_s	Nominal settling time	30 s
t_T	Total simulation time	320 s
k	Nominal proportional gain	$0.2957(I^3)$
i	Nominal integral gain	$0.0003(I^3)$
d	Nominal derivative gain	$0.0011(I^3)$
Λ	Unknown control effectiveness	$0.75(I^3)$
W_p	Unknown weight matrix	$-[0.25(I^3) \quad 0.6(I^3)]^T$
γ	Adaptation gain	10
ϵ	System error performance	3×10^{-4}
κ	Leakage term	$[5 \quad 4.8 \quad 2.5]^T$

TABLE 4. Offset vector estimation.

#	$\tilde{r}_{CM_x}(\mu m)$	$\tilde{r}_{CM_y}(\mu m)$	$\tilde{r}_{CM_z}(\mu m)$
0	0.0	0.0	0.0
1	−0.06333334361899	0.47466674375496	−3.32000053918478
2	−0.11400003332555	0.85440024976625	−5.97600174695949
3	−0.08550001874562	0.64080014049349	−4.48200098266459
4	−0.09690002407771	0.72624018045610	−5.07960126217815
5	−0.09490502309648	0.71128817310202	−4.97502121074100
6	−0.09500002314273	0.71200017344866	−4.98000121316577

TABLE 5. Moving mass position.

#	$r_{m_x}(\text{mm})$	$r_{m_y}(\text{mm})$	$r_{m_z}(\text{mm})$
0	0.0	0.0	0.0
1	−0.0016213335966462	0.0121514686401269	−0.076492812422817
2	−0.002918400853134	0.021872646394016	−0.137687080249947
3	−0.002188800479888	0.016404483596633	−0.103265302640592
4	−0.002480640616389	0.018591748619676	−0.117034013080584
5	−0.002429568591270	0.018208977231412	−0.114624488695473
6	−0.002432000592454	0.018227204440286	−0.114739227951339

Once the static unbalance is handled by the movable masses and the angular motion is reduced below 0.01 degree with a pendulum period over 100 seconds, we proceed with the next part of the scheme, the simulation of the implemented MRAC, used to counteract the parameter uncertainty and unknown perturbation so that to improve the system performance.

For this part of the scheme, the control parameters, Table 3, used in the adaptive control architecture were designed according to the nominal control law and the system error performance for a strict bounded system error, getting defined command tracking accuracy and improved attitude stability.

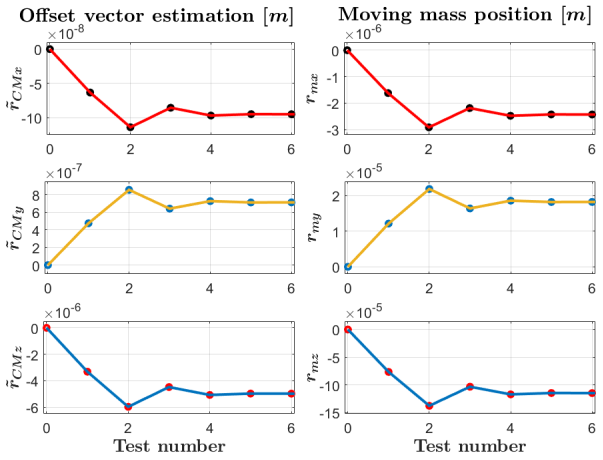

FIGURE 2. Vector offset estimation and moving mass position for each iteration time.

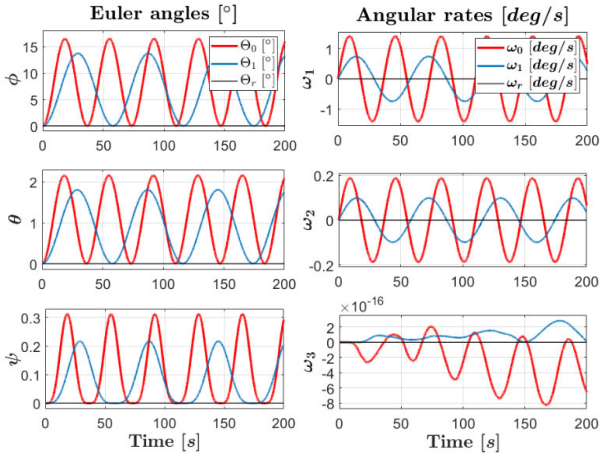

FIGURE 3. Euler angles, and angular rates response (Initial, and first-time least square batch estimation).

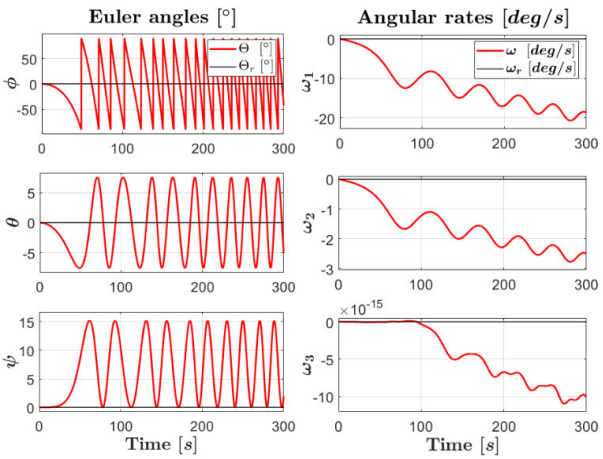

FIGURE 4. Euler angles, and angular rates response (Second-time least square batch estimation).

In simulations, it was assumed that the control actuators were not performing ideally. In consequence, the control effectiveness be reduced to a 75% of their capacity.

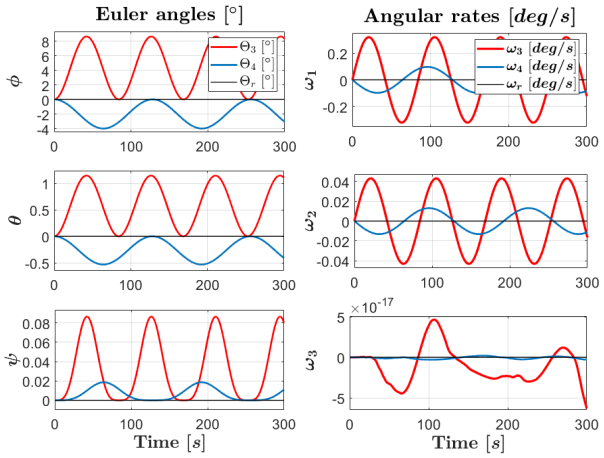

FIGURE 5. Euler angles, and angular rates response (third-, and fourth-time least square batch estimation).

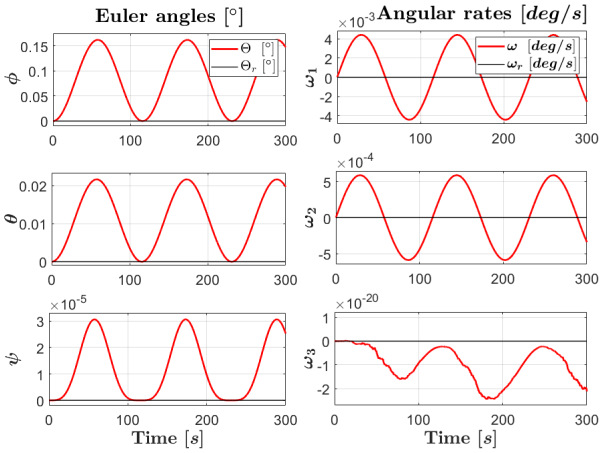

FIGURE 6. Euler angles, and angular rates response (Fifth-time least square batch estimation).

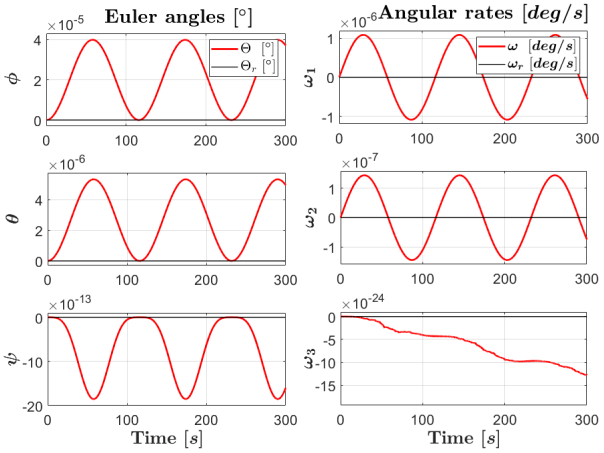

FIGURE 7. Euler angles, and angular rates response (Sixth-time least square batch estimation).

Consider that in this part of the numerical simulation, static unbalance due to the offset vector $\boldsymbol{r_{CM}}$ defined in section III-B, had been counteracted by the moving masses, keeping a remaining estimated offset vector $\tilde{\boldsymbol{r}}_{\boldsymbol{CM_6}}$ (Table 4) used in the dynamic equations of motion as another external perturbation according to the gravitational torque defined in (51). which can be rewritten into (52) by considering the Euler parameter representation and applying the small angle assumption.

$$\boldsymbol{\tau_g} = M_s g \begin{bmatrix} -r_y \cos\phi\cos\theta + r_z \sin\phi\cos\theta \\ r_x \cos\phi\cos\theta + r_z \sin\theta \\ -r_x \sin\phi\cos\theta - r_y \sin\theta \end{bmatrix} \tag{51}$$

$$\boldsymbol{\tau_g} = M_s g \begin{bmatrix} -r_y + r_z\,(4q_2q_3 - 2q_1) \\ r_x + r_z\,(-2q_2 - 4q_1q_3) \\ -r_x\,(4q_2q_3 - 2q_1) - r_y\,(-2q_2 - 4q_1q_3) \end{bmatrix} \tag{52}$$

Now, in order to simulate space environment conditions acting on the attitude simulator system, uniform random signals are introduced as external momentum exchange $\left(\boldsymbol{\tau_d} = \pm\text{rand}\left(\begin{bmatrix}0.5 & 0.5 & 0.5\end{bmatrix}^T\right) \times 10^{-5}\text{N·m}\right)$.

In addition, the generated gravitational torque is added to this external uniform random signal to be counted as the total perturbation acting on the system $\boldsymbol{\tau_{total}} = \left(\boldsymbol{\tau_g} + \boldsymbol{\tau_d}\right)$.

TABLE 6. Period estimation vs period response.

#	T (s)	$\tilde{T}$ (s)	max(Eul) (°)
0	36.5007083888843	36.75	16.4197699867824
1	44.7040554014461	45.01	13.6738644224605
2	NaN	NaN	NaN
3	84.1678448004092	84.21	8.62812007765469
4	129.204590291909	128.15	3.99653355102708
5	116.151745788778	115.53	0.162333274720998
6	116.68595469575	116.02	0.000039911239569

Assume that linear equations of motion were considered for numerical simulations of the attitude simulator with the MRAC approach (Appendix A) [53].

Parameters, initial conditions, and simulation setup are taken according to Table 2 and Table 3. In addition, let the reference command be set by (53), where $\boldsymbol{c}(t) = \begin{bmatrix}\phi & \theta & \psi\end{bmatrix}^T$ are the set of Euler angles in the following command.

$$\boldsymbol{c}(t) = \begin{cases} \begin{bmatrix}3.5°, & 5°, & 6.5°\end{bmatrix}^T, & 50 > t \geq 0 \\ \begin{bmatrix}1°, & -1.5°, & -0.5°\end{bmatrix}^T, & 100 > t \geq 50 \\ \begin{bmatrix}2°, & 3°, & 5°\end{bmatrix}^T, & 150 > t \geq 100 \\ \begin{bmatrix}0°, & 0°, & 0°\end{bmatrix}^T, & 200 > t \geq 150 \\ \begin{bmatrix}1.5°, & 2.5°, & 4°\end{bmatrix}^T, & 250 > t \geq 200 \\ \begin{bmatrix}1°, & 2°, & 3°\end{bmatrix}^T, & 320 > t \geq 250 \end{cases} \tag{53}$$

VI. RESULTS AND DISCUSSION

This section is divided into two parts. The first part shows simulation results after performing automatic mass balancing of the attitude simulator in order to reduce the offset vector

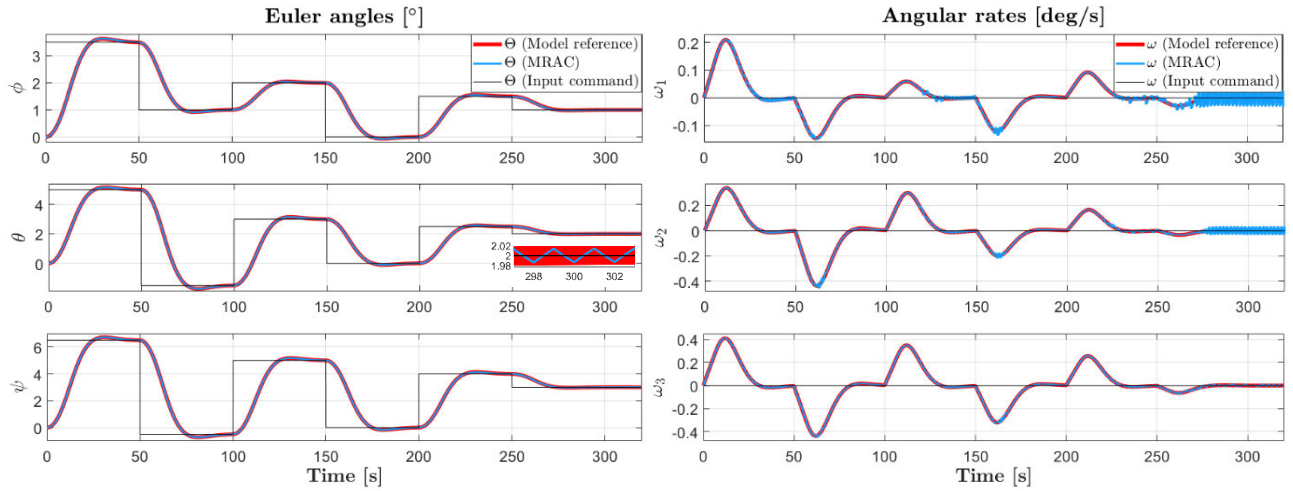

FIGURE 8. Euler angles, and angular rates response to the MRAC with user-defined performance.

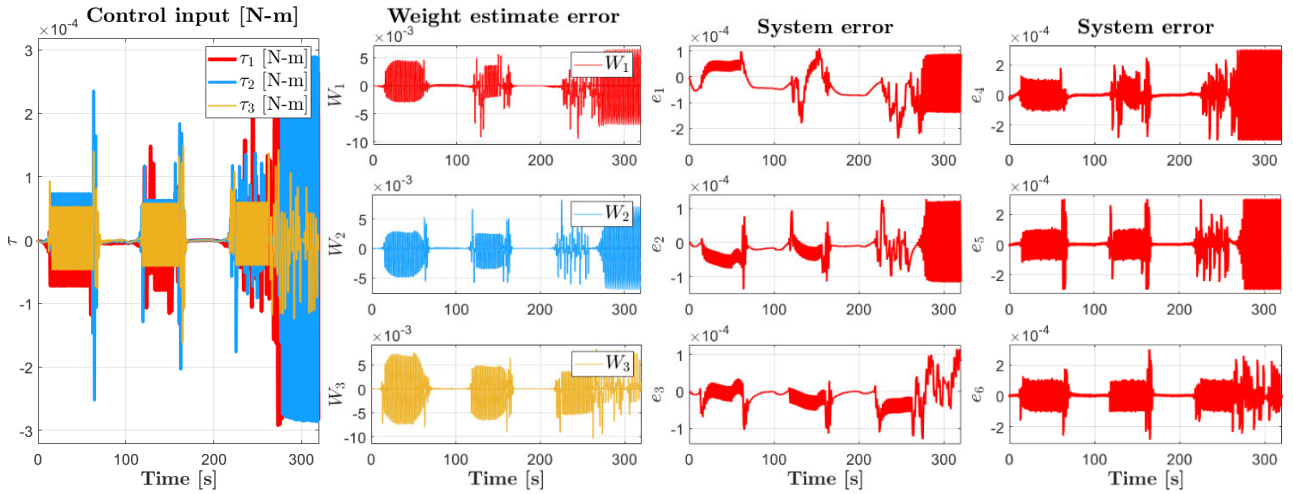

FIGURE 9. Control input, weight estimate error, and System error response to the MRAC with user-defined performance.

$\boldsymbol{r_{CM}}$. The second part shows simulation results of the MRAC for improved system performance.

A. OFFSET VECTOR ESTIMATION AND MOVING MASS POSITION

By definition, the travelling distance r_{m_i} is in direct relationship with the offset vector in the automatic mass balancing method (13). Hence, according to Fig. 2, the changes in the estimated offset vector $\tilde{\boldsymbol{r}}_{\boldsymbol{CM}}$ is varying according to the position of the moving mass along the principal axis of the simulator. Estimated values for $\tilde{\boldsymbol{r}}_{\boldsymbol{CM}}$ corresponding to the traveled distance by $\boldsymbol{r_{m_i}}$, at each iteration time (1 to 6) are presented in Table 4 and Table 5, respectively.

Fig. 3 to Fig. 7 show numerical simulation results after performing the least square batch estimation of the offset vector $\boldsymbol{r_{CM}}$ at each iteration time. According to Fig. 3, the initial response of the pendulum-like motion caused by the initial offset vector is expressed by the set of Euler angles $\boldsymbol{\Theta_0}$ and set of angular rates $\boldsymbol{\omega_0}$ (Time 0). Then, for the same figure, the first–time response of the automatic travelling distance of the movable masses (distance $\Delta\boldsymbol{r_m}$) are according to the first estimation of the offset vector (14), and it is expressed by the Euler angle $\boldsymbol{\Theta_1}$ and angular rate $\boldsymbol{\omega_1}$ (Time 1).

In a similar fashion, the second-time response of the automatic least square batch estimation method can be obtained by performing new travelling distances by the movable masses according to the second-time estimation of the vector offset, but with a peculiar motion behavior, Fig. 4.

This unstable behavior may occur due to the excessive travelling distance of the movable mass, especially in case the travelled distance of the movable mass along the $z-$axis makes the offset vector rotate in the opposite direction; hence its change in sign, making the pendulum-like motion of the system perform as an inverted pendulum-like motion. To this point it may be required to return the movable masses to a

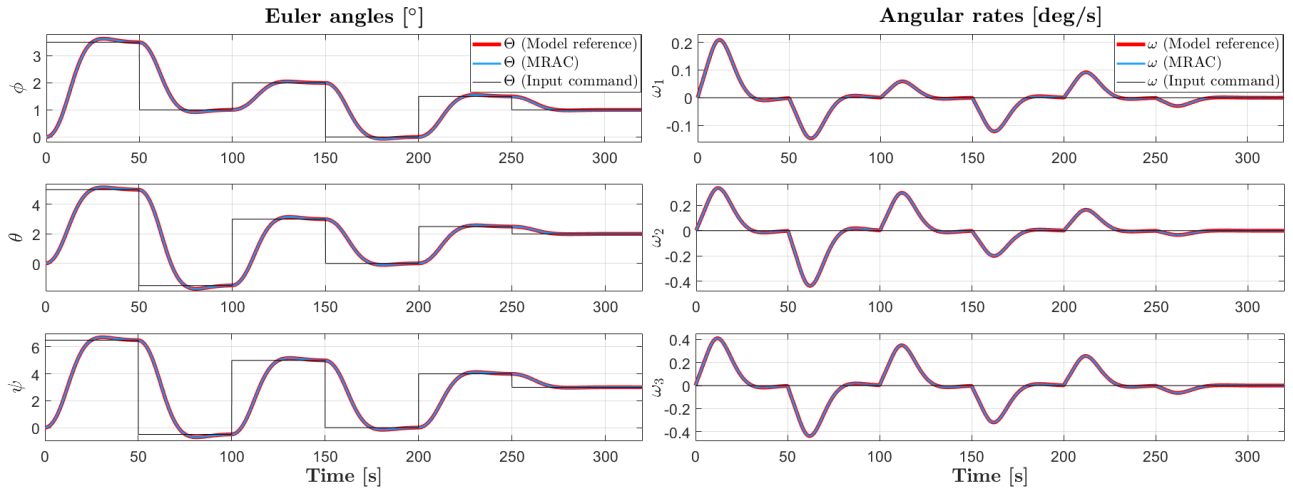

FIGURE 10. Euler angles, and angular rates response to the modified adaptive control input design.

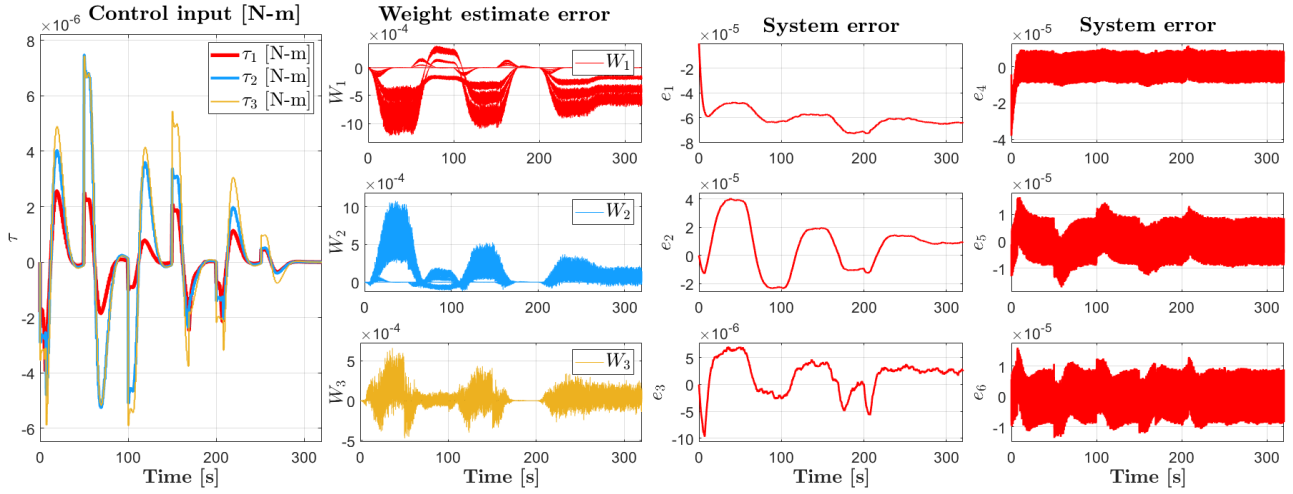

FIGURE 11. Control input, weight estimate error, and System error response to the modified adaptive control input design.

previous position before performing the next batch estimation iteration.

Fig. 5 and Fig. 6 show the motion response for the following batch estimation iterations. Note that each time, the estimated offset vector $\boldsymbol{r}_{\tilde{CM}}$ is getting close to the real offset vector r_{CM} the period of the pendulum-like motion is increased, while the amplitude of oscillations in the Euler angles decreases at each iteration time.

Numerical simulation results of the estimated period $\tilde{T}$, remark 1, and maximum value of amplitude in the oscillations of the Euler angles, max(Eul), are shown in Table 6 for each iteration time. A comparison between the estimated period $\tilde{T}$ and the calculated period T, (15), can be conducted to validate the batch estimation method.

Note that, while a fine offset vector estimation can be obtained with numerical simulations by implementing the least square batch estimation method, in real implementation, it would be hard to achieve such performance. This is due to the short travelling distance a movable mass should carry out each iteration time. Since the travelling distance $\boldsymbol{r}_{m_i}$ is in direct relationship with each individual mass m_i, a possible solution is to select smaller travelling masses along the axes. Especial care must be taken at the moment of selecting and adopting the mechanical design of an attitude simulator.

B. MRAC WITH USER-DEFINED PERFORMANCE AND IMPROVED ADAPTIVE INPUT ERROR MODIFICATION

In the last part of this section, simulation results under user-defined performance MRAC, (Fig. 8, and Fig. 9), and input error modification (Fig. 10, and Fig. 11) schemes are presented.

Fig. 8, and Fig. 9 show simulation results of the adopted MRAC with user-defined performance presented in Section III. It can be seen that while the attitude accuracy remains acceptable for a remote sensing small satellite $< 0.1°$ (at settling time), the attitude stability reaches its limits with

an approximate maximum value ≈ 0.0325deg/s (considering that a satellite mission design may constrain this parameter below 0.05deg/s).

As mentioned in a previous section, this attitude stability behavior may occur due to the system design itself. Another possible cause is the selection of the leakage term. Note their values in Table 3, and consider that for greater values of this term, the oscillations in the second state are increased as well. While it may seem that a smaller value of the leakage term provides a better response, this term is linked to the weight estimation error dynamics (34), hence, the system error dynamics (28), hence, the adaptive law (30) (Fig. 9), in consequence to the robustness and attitude accuracy itself.

Note that while, for bigger values of κ we can get better results in accuracy, smaller values of it will deliver better attitude stability in a trade-off condition. Especial care in choosing a bigger value of the leakage term must be considered since it may prevent adaptation in the weight estimation error dynamics (34). In addition, in Fig. 9, we can see that the system errors reach their boundaries more easily according to the parameter of the error performance ϵ for bigger values of κ.

Finally, the results of the proposed MRAC with error input modification show improved attitude stability while keeping acceptable attitude accuracy, Fig. 10.

Note in Fig. 11 that for the same simulation conditions as in previous MRAC scheme, the weight estimation error, and the system error are one order of magnitude below, while having smooth control input signals, making it more suitable for hardware implementation.

VII. CONCLUSION AND FUTURE WORK

A. CONCLUSION

This paper presents a comprehensive approach to enhance the performance of a small spherical attitude simulator, suitable for verification of attitude control algorithms, particularly focusing on small satellites 1U-class CubeSat platform. The main contributions of this work are centred on developing an automatic mass balancing system by performing the least-squares batch estimation method followed by a modified Model Reference Adaptive Control (MRAC) with modified architecture to address uncertain suppression and perturbation rejection. In this research, for the addressed spherical attitude simulator, we presented a reduced dynamical equation of motion with Euler parameters representation used in the batch estimation method, reducing significantly the computational complexity at the moment of performing the automatic mass balancing of the system. Method which effectively estimates and mitigates the offset vector caused by the mass imbalance of the system, where small masses along the principal axes dynamically adjust their position to enhance system stability and reduce static unbalance. Then, a modified MRAC with user-defined performance architecture with input error modification is incorporated into the scheme to counteract dynamic unbalance, improving significantly the performance and attitude stability of the system. The adaptive controller effectively counteracts parametric uncertainties and unknown external disturbances, ensuring robustness in the attitude control of the simulator. Finally, the effectiveness of the proposed method is validated with extensive numerical simulations where the results indicate that the automatic mass balancing system, combined with the modified MRAC, provides superior performance in terms of stability and accuracy, making it suitable for hardware implementation.

B. FUTURE WORKS

Future research directions will focus on experimental validation by implementing the proposed method into the physical spherical attitude simulator to validate the simulation results with real-time implementation and hardware integration to enable on-the-fly adjustments and corrections during attitude control tasks. One point of interest is to investigate the scalability and adaptability of the proposed method for larger satellites with different types of attitude simulators, ensuring its adaptability to the different control mission requirements and environmental conditions. Address advanced disturbance rejection techniques to further enhance the robustness and reliability of the attitude control system under challenging conditions.

APPENDIX A

Nominal state space representation of the attitude simulator dynamics:

$$\begin{aligned}\begin{bmatrix}\dot{\boldsymbol{q}}\\ \dot{\boldsymbol{\omega}}\end{bmatrix} &= \begin{bmatrix} g\left(\boldsymbol{q},\omega\right)\\ J_s^{-1} f\left(\boldsymbol{\omega}, h^b\right)\end{bmatrix} + \begin{bmatrix} 0_3\\ J_s^{-1}\end{bmatrix}\boldsymbol{u}^b + \boldsymbol{\tau_d}\\ &= A + Bu^b + \tau_d \qquad \text{(A1)}\\ \boldsymbol{y} &= \begin{bmatrix}\boldsymbol{q}\\ \boldsymbol{\omega}\end{bmatrix}^+ = \begin{bmatrix} I^3 & 0^{3\times 3}\end{bmatrix}\begin{bmatrix}\boldsymbol{q}\\ \boldsymbol{\omega}\end{bmatrix} + \begin{bmatrix}0^{3\times 3}\end{bmatrix}\boldsymbol{u^b}\\ &= Cx + D\boldsymbol{u}^b\\ \boldsymbol{x} &= \begin{bmatrix}\boldsymbol{q} & \boldsymbol{\omega}\end{bmatrix}^T \qquad \text{(A2)}\end{aligned}$$

Linearized state space representation:

$$A = \begin{bmatrix} 0 & 0 & 0 & 0.5 & 0 & 0\\ 0 & 0 & 0 & 0 & 0.5 & 0\\ 0 & 0 & 0 & 0 & 0 & 0.5\\ f_{41} & 0 & 0 & 0 & 0 & f_{46}\\ 0 & f_{52} & 0 & 0 & 0 & 0\\ 0 & 0 & f_{63} & f_{64} & 0 & 0\end{bmatrix} \qquad \text{(A3)}$$

$$B = \begin{bmatrix} 0 & 0 & 0\\ 0 & 0 & 0\\ 0 & 0 & 0\\ J_{11}^{-1} & 0 & 0\\ 0 & J_{22}^{-1} & 0\\ 0 & 0 & J_{33}^{-1}\end{bmatrix}$$

$$diag\left(J_s\right) = \begin{bmatrix} J_{11} & J_{22} & J_{33}\end{bmatrix}^T \qquad \text{(A4)}$$

$$f_{41} = -8\omega_0^2 K_1, \quad f_{63} = -2\omega_0^2 K_3 \qquad \text{(A5)}$$

$$f_{46} = \omega_0 (1 - K_1), \quad f_{64} = -\omega_0 (1 - K_3) \tag{A6}$$

$$f_{52} = -6\omega_0^2 K_2 \tag{A7}$$

$$K_1 = \frac{(J_{22} - J_{33})}{J_{11}}, \quad K_2 = \frac{(J_{11} - J_{33})}{J_{22}},$$
$$K_3 = \frac{(J_{22} - J_{11})}{J_{33}} \tag{A8}$$

ACKNOWLEDGMENT

The authors would like to thank the Instituto de Investigación Astronómico y Aeroespacial Pedro Paulet (IAAPP-UNSA), Universidad Nacional de San Agustín de Arequipa and Beihang University, for making this research possible.

REFERENCES

[1] G. A. Smith, "Dynamic simulation for test of space vehicle attitude control systems," in *Proc. Conf. Role Simulation Space Technol.* Blacksburg, VA, USA: Virginia Polytechnic Inst. State University, 1964, pp. XI-1–XV-30.

[2] G. Sharifi, M. Mirshams, and H. S. Ousaloo, "Mass properties identification and automatic mass balancing system for satellite attitude dynamics simulator," *Proc. Inst. Mech. Eng., G, J. Aerosp. Eng.*, vol. 233, no. 3, pp. 896–907, Dec. 2017, doi: 10.1177/0954410017742932.

[3] J. L. Schwartz and C. D. Hall, "System identification of a spherical air-bearing spacecraft simulator," in *Proc. AAS/AIAA Space Flight Mech. Conf.*, vol. 122, 2004, pp. 8–12.

[4] S. Chesi, Q. Gong, V. Pellegrini, R. Cristi, and M. Romano, "Automatic mass balancing of a spacecraft three-axis simulator: Analysis and experimentation," *J. Guid., Control, Dyn.*, vol. 37, no. 1, pp. 197–206, Jan. 2014, doi: 10.2514/1.60380.

[5] J. J. Kim and B. Agrawal, "System identification and automatic mass balancing of ground-based three-axis spacecraft simulator," in *Proc. AIAA Guid., Navigat., Control Conf. Exhib.*, Aug. 2006, pp. 4224–4235.

[6] J. J. Kim and B. N. Agrawal, "Automatic mass balancing of air-bearing-based three-axis rotational spacecraft simulator," *J. Guid., Control, Dyn.*, vol. 32, no. 3, pp. 1005–1017, May 2009, doi: 10.2514/1.34437.

[7] R. C. da Silva, R. A. Borges, S. Battistini, and C. Cappelletti, "A review of balancing methods for satellite simulators," *Acta Astronautica*, vol. 187, pp. 537–545, Oct. 2021, doi: 10.1016/j.actaastro.2021.05.037.

[8] D. Modenini, A. Bahu, G. Curzi, and A. Togni, "A dynamic testbed for nanosatellites attitude verification," *Aerospace*, vol. 7, no. 3, p. 31, Mar. 2020, doi: 10.3390/aerospace7030031.

[9] S. Jamshidi, M. Mirzaei, and M. Malekzadeh, "Applied nonlinear control of spacecraft simulator with constraints on torque and momentum of reaction wheels," *ISA Trans.*, vol. 138, pp. 705–719, Jul. 2023, doi: 10.1016/j.isatra.2023.03.027.

[10] M. Malekzadeh and H. Sadeghian, "Attitude control of spacecraft simulator without angular velocity measurement," *Control Eng. Pract.*, vol. 84, pp. 72–81, Mar. 2019, doi: 10.1016/j.conengprac.2018.11.011.

[11] J. Prado, G. Bisiacchi, L. Reyes, E. Vicente, F. Contreras, M. Mesinas, and A. Juárez, "Three-axis air-bearing based platform for small satellite attitude determination and control simulation," *J. Appl. Res. Technol.*, vol. 3, no. 3, pp. 222–237, Dec. 2005, doi: 10.22201/icat.16656423.2005.3.03.563.

[12] K. Saulnier, D. Pérez, R. C. Huang, D. Gallardo, G. Tilton, and R. Bevilacqua, "A six-degree-of-freedom hardware-in-the-loop simulator for small spacecraft," *Acta Astronautica*, vol. 105, no. 2, pp. 444–462, Dec. 2014, doi: 10.1016/j.actaastro.2014.10.027.

[13] S. Chesi, Q. Gong, O. Perez, and M. Romano, "A dynamic, hardware-in-the-loop, three-axis simulator of spacecraft attitude maneuvering with nanosatellite dimensions," *J. Small Satell.*, vol. 4, no. 1, pp. 315–328, 2015.

[14] D. Jung and P. Tsiotras, "A 3-DoF experimental test-bed for integrated attitude dynamics and control research," in *Proc. AIAA Guid., Navigat., Control Conf. Exhib.*, Jun. 2003, pp. 5331–5341, doi: 10.2514/6.2003-5331.

[15] R. C. da Silva, I. S. K. Ishioka, C. Cappelletti, S. Battistini, and R. A. Borges, "Helmholtz cage design and validation for nanosatellites HWIL testing," *IEEE Trans. Aerosp. Electron. Syst.*, vol. 55, no. 6, pp. 3050–3061, Dec. 2019, doi: 10.1109/TAES.2019.2898309.

[16] J. S. Young, "Balancing of a small satellite attitude control simulator on an air bearing," in *Proc. Utah Space Grant Consortium Symp.*, Salt Lake City, UT, USA, Jan. 1998.

[17] J. L. Schwartz, M. A. Peck, and C. D. Hall, "Historical review of air-bearing spacecraft simulators," *J. Guid., Control, Dyn.*, vol. 26, no. 3, pp. 513–522, May 2003, doi: 10.2514/1.1035.

[18] R. F. Costa, O. Saotome, and E. Rafikova, "Simulation and validation of satellite attitude control algorithms in a spherical air bearing," *J. Control, Autom. Electr. Syst.*, vol. 30, no. 5, pp. 716–727, Jul. 2019, doi: 10.1007/s40313-019-00497-4.

[19] M. Golestani, K. A. Alattas, S. U. Din, S. Mobayen, A. K. Alanazi, and A. Fekih, "A simple structure constrained attitude control for rigid bodies: A PD-type control," *IEEE Access*, vol. 10, pp. 10202–10209, 2022, doi: 10.1109/ACCESS.2022.3144627.

[20] R. Kristiansen and P. J. Nicklasson, "Satellite attitude control by quaternion-based backstepping," in *Proc., Amer. Control Conf.*, 2005, pp. 907–912, doi: 10.1109/acc.2005.1470075.

[21] J. H. McDuffie and Y. B. Shtessel, "A de-coupled sliding mode controller and observer for satellite attitude control," in *Proc. 29th Southeastern Symp. Syst. Theory*, Mar. 1997, pp. 92–97, doi: 10.1109/SSST.1997.581585.

[22] B. Wie, H. Weiss, and A. Arapostathis, "Quarternion feedback regulator for spacecraft eigenaxis rotations," *J. Guid., Control, Dyn.*, vol. 12, no. 3, pp. 375–380, May 1989, doi: 10.2514/3.20418.

[23] E. Arabi and T. Yucelen, "Experimental results with the set-theoretic model reference adaptive control architecture on an aerospace testbed," in *Proc. AIAA Scitech Forum*, Jan. 2019, pp. 930–945, doi: 10.2514/6.2019-0930.

[24] D.-W. Zhang, G.-P. Liu, and L. Cao, "Predictive control of discrete-time high-order fully actuated systems with application to air-bearing spacecraft simulator," *J. Franklin Inst.*, vol. 360, no. 8, pp. 5910–5927, May 2023, doi: 10.1016/j.jfranklin.2023.04.003.

[25] W. MacKunis, K. Dupree, S. Bhasin, and W. E. Dixon, "Adaptive neural network satellite attitude control in the presence of inertia and CMG actuator uncertainties," in *Proc. Amer. Control Conf.*, Jun. 2008, pp. 2975–2980, doi: 10.1109/acc.2008.4586948.

[26] J. G. Webster and T. Yucelen, "Model reference adaptive control," in *Wiley Encyclopedia of Electrical and Electronics Engineering*. Hoboken, NJ, USA: Wiley, 2024, doi: 10.1002/047134608X.W1022.pub2.

[27] E. Arabi, B. C. Gruenwald, T. Yucelen, and N. T. Nguyen, "A set-theoretic model reference adaptive control architecture for disturbance rejection and uncertainty suppression with strict performance guarantees," *Int. J. Control*, vol. 91, no. 5, pp. 1195–1208, Apr. 2017, doi: 10.1080/00207179.2017.1312019.

[28] D. Long, X. Wen, W. Zhang, and J. Wang, "Recurrent neural network based robust actuator and sensor fault estimation for satellite attitude control system," *IEEE Access*, vol. 8, pp. 183165–183174, 2020, doi: 10.1109/ACCESS.2020.3029066.

[29] F. L. Markley and J. L. Crassidis, *Fundamentals of Spacecraft Attitude Determination and Control*. New York, NY, USA: Springer, 2014.

[30] M. J. Sidi, *Spacecraft Dynamics and Control: A Practical Engineering Approach*. Cambridge, U.K.: Cambridge Univ. Press, 2006.

[31] R. A. Serway and J. W. Jewett, *Physics for Scientists and Engineers*. Pacific Grove, CA, USA: Cengage Learning, 2010.

[32] B. Wie, *Space Vehicle Dynamics and Control*. Reston, VA, USA: American Institute of Aeronautics and Astronautics, 2008.

[33] J. R. Wertz, *Spacecraft Attitude Determination and Control*. Dordrecht, The Netherlands: Springer, 2012.

[34] D. T. Greenwood, *Principles of Dynamics*. Englewood Cliffs, NJ, USA: Prentice-Hall, 1988.

[35] P. A. Ioannou and S. Jing, *Robust Adaptive Control*. Upper Saddle River, NJ, USA: Prentice-Hall, 1996.

[36] E. Lavretsky and K. A. Wise, *Robust and Adaptive Control* (Advanced Textbooks in Control and Signal Processing). London, U.K.: Springer, 2013, doi: 10.1007/978-1-4471-4396-3.

[37] K. S. Narendra and A. M. Annaswamy, *Stable Adaptive Systems*. North Chelmsford, MA, USA: Courier Corporation, 2012.

[38] T. Yucelen and J. S. Shamma, "Adaptive architectures for distributed control of modular systems," in *Proc. Amer. Control Conf.*, Jun. 2014, pp. 1328–1333, doi: 10.1109/ACC.2014.6858859.

[39] A. K. Kostarigka and G. A. Rovithakis, "Adaptive dynamic output feedback neural network control of uncertain MIMO nonlinear systems with prescribed performance," *IEEE Trans. Neural Netw. Learn. Syst.*, vol. 23, no. 1, pp. 138–149, Jan. 2012, doi: 10.1109/TNNLS.2011.2178448.
[40] B. Ren, S. S. Ge, K. P. Tee, and T. H. Lee, "Adaptive neural control for output feedback nonlinear systems using a barrier Lyapunov function," *IEEE Trans. Neural Netw.*, vol. 21, no. 8, pp. 1339–1345, Aug. 2010, doi: 10.1109/TNN.2010.2047115.
[41] K. Peng Tee, S. S. Ge, and F. E. H. Tay, "Adaptive control of electrostatic microactuators with bidirectional drive," *IEEE Trans. Control Syst. Technol.*, vol. 17, no. 2, pp. 340–352, Mar. 2009, doi: 10.1109/TCST.2008.2000981.
[42] K. P. Tee, S. S. Ge, and E. H. Tay, "Barrier Lyapunov functions for the control of output-constrained nonlinear systems," *Automatica*, vol. 45, no. 4, pp. 918–927, Apr. 2009, doi: 10.1016/j.automatica.2008.11.017.
[43] K. B. Ngo, R. Mahony, and Z.-P. Jiang, "Integrator backstepping using barrier functions for systems with multiple state constraints," in *Proc. 44th IEEE Conf. Decis. Control*, Dec. 2005, pp. 8306–8312, doi: 10.1109/CDC.2005.1583507.
[44] J.-J. E. Slotine and W. Li, *Applied Nonlinear Control: An Introduction*. Englewood Cliffs, NJ, USA: Prentice-Hall, 1991.
[45] B. Wie and P. Barba, "Quaternion feedback for spacecraft large angle maneuvers," in *Proc. 25th Struct., Structural Dyn. Mater. Conf.*, May 1984, pp. 360–365, doi: 10.2514/6.1984-1032.
[46] B. Wie, D. Bailey, and C. Heiberg, "Rapid multitarget acquisition and pointing control of agile spacecraft," *J. Guid., Control, Dyn.*, vol. 25, no. 1, pp. 96–104, Jan. 2002, doi: 10.2514/2.4854.
[47] W. Hu, *Fundamental Spacecraft Dynamics and Control*. Hoboken, NJ, USA: Wiley, 2015.
[48] H. D. Curtis, *Orbital Mechanics for Engineering Students*. Oxford, U.K.: Butterworth-Heinemann, 2021.
[49] S. Blažič, I. Škrjanc, and D. Matko, "Adaptive law with a new leakage term," *IET Control Theory Appl.*, vol. 4, no. 9, pp. 1533–1542, Sep. 2010, doi: 10.1049/iet-cta.2009.0349.
[50] P. R. Yanyachi, H. Mamani-Valencia, and B. Espinoza-García, "Low-cost test system for 1U CubeSat attitude control with reaction wheels," in *Proc. IEEE Biennial Congr. Argentina (ARGENCON)*, Sep. 2022, pp. 1–8, doi: 10.1109/ARGENCON55245.2022.9940099.
[51] B. E. Garcia, A. Martin, and P. Raul, "Non-linear control strategies for attitude maneuvers in a CubeSat with three reaction wheels," *Int. J. Adv. Comput. Sci. Appl.*, vol. 11, no. 11, pp. 728–737, 2020, doi: 10.14569/ijacsa.2020.0111189.
[52] A. Mamani-Saico and P. R. Yanyachi, "Implementation and performance study of the micro-ROS/ROS2 framework to algorithm design for attitude determination and control system," *IEEE Access*, vol. 11, pp. 128451–128460, 2023, doi: 10.1109/ACCESS.2023.3330441.
[53] Y. Yang, "Spacecraft attitude determination and control: Quaternion based method," *Annu. Rev. Control*, vol. 36, no. 2, pp. 198–219, Dec. 2012, doi: 10.1016/j.arcontrol.2012.09.003.

JAIME GERSON CUBA MAMANI received the B.Sc. degree in electronic engineering from Universidad Nacional de San Agustín de Arequipa, Arequipa, Peru, in 2014, and the M.Sc. degree in space technology applications (micro-satellite technology) from Beihang University, Beijing, China, by the Regional Centre for Space Science and Technology Education in Asia and the Pacific, China, through the Asia-Pacific Space Cooperation Organization (APSCO), in 2019. From 2014 to 2017, he participated as a Research Assistant and a Junior Programmer in research projects with the Astronomical and Aerospace Institute Pedro Paulet, National University of San Agustin of Arequipa. His research interests include small satellite technology, guidance, navigation, attitude estimation, attitude control, and learning and intelligent control.

XINSHENG WANG received the M.Sc. degree in control theory and control engineering from the Chinese Academy of Space Technology (CAST), in 2001, and the Ph.D. degree in signal and information processing from Beijing University of Post and Telecommunication (BUPT), Beijing, China, in 2005. In 2003, he worked at EADS Space Transportation as an Associate Researcher. He pursued micro-satellite project work at Shenzhen Space Technology Center (SSTC), Shenzhen, China, from 2004 to 2007. From 2006 to 2008, he was a Postdoctoral Researcher. He is currently a Faculty Member with the Department of Spacecraft Technology, School of Astronautics, Beihang University. His research interests include micro-satellite system engineering technology, satellite OBDH systems, spacecraft fault detection, and diagnosis technology.

PABLO RAUL YANYACHI (Senior Member, IEEE) received the M.Sc. degree in automatic control from the Polytechnic Institute of Leningrad and the Ph.D. degree in electrical engineering from the Polytechnic School, University of São Paulo, Brazil. He is currently a main Professor with the Department of Electronic Engineering, Universidad Nacional de San Agustín de Arequipa (UNSA), Arequipa, Peru. He is the Station Manager of the NASA Laser Tracking Station TLRS-3, Arequipa. He is also the Director of the Instituto de Investigación Astronómico y Aeroespacial Pedro Paulet (IAAPP), UNSA.